6ICEGE 6th International Conference on Earthquake Geotechnical Engineering
1-4 November 2015
Christchurch, New Zealand

Seismic Response of Sedimentary Basin Subjected to Obliquely Incident SH Waves

C. B. Zhu[1], D.P. Thambiratnam[2], J. Zhang[3]

ABSTRACT

This article studies the impact of the incident angle of *SH* waves on the seismic response of a sedimentary basin using two-dimensional nonlinear seismic response analysis. Ricker waves with different incident angles, Peak Ground Accelerations (*PGA*s) and predominant frequencies are considered. Results show that the amplification ratio of acceleration varies with the incident angle of *SH* waves and that the maximum ratio does not occur necessarily for vertically incident *SH* waves, but for incident angles approximately in the range 0° to 25°. The increase in the predominant frequency of incident *SH* waves reduces the range of incident angle that has an effect on *PGA*. The slope angle of the basin has a significant influence on the distribution pattern of *PGA*s along the basin surface; the strongest-response position shifts gradually from the edge towards the center of a basin with the increase of slope angle.

Introduction

The seismic response of a site is affected by many factors, such as source characteristics, propagation path and local site conditions. Among all these factors, local site conditions (Borcherdt and Glassmoyer, 1992) have a particularly significant impact on the seismic site response, these effects caused by local site condition are well known among the geotechnical engineers and seismologists as site effect. Local site conditions may cause significant amplification of ground motion and concentrated damage during an earthquake (Assimaki and Gazetas, 2004).

The basin-effect (Choi Y. et al., 2005) has been recognized by researchers for several years as one kind of site effect, for example, the 2012 Christchurch earthquake further confirmed the amplification effect of basin (Cubrinovski, M. and Green R. A., 2010). The seismic response of a basin will be determined by both the characteristics of the basin (including both the geometric and the geotechnical parameters) and the input motion (like incident angle, amplitude, spectral characteristic and duration) regardless of the impacts of the source characteristic and propagation path.

[1]PhD candidate CB Zhu, Scienece and Engineering Faculty, Queensland University of Technology, Brisbane, Australia, chuanbin.zhu@hdr.qut.edu.au
[2]Professor DP Thambiratnam, Scienece and Engineering Faculty, Queensland University of Technology, Brisbane, Australia, d.thambiratnam@qut.edu.au
[3]Professor J. Zhang, School of Civil Engineering, Southwest Jiaotong University, Chengdu, China, jianzhang1102@home.swjtu.edu.cn

Several researchers have extensively investigated the effects of different parameters on the seismic response of a basin or valley. This includes studies on the following parameters: nonlinear soil property (Jian Zhang, 2008; Gelagoti F., 2012), filling ratio (Behrouz Gatmiri and Talat Foroutan, 2012), impedance contract (Behrouz Gatmiri and Talat Foroutan, 2012), resonance (Thomas L. Pratt, 2003), conversion of body waves to surface waves at the edge of basin (Brian M. Adams et al., 2003), shape ratio (half width to the depth of a basin) (Gelagoti F., 2012). In most of the above studies, vertically incident waves were considered. However, seismic waves can reach the ground obliquely as a result of the complexity of the wave propagation path and the topography (Takahiro Sigaki, 2000). It is hence important to study the seismic response of sediment-filled basin or valley subjected to obliquely incident body waves (You H. B. et al., 2009).

In the present paper, the impact of the geometry parameters of a basin on its seismic response and the characteristic of the incident seismic waves, especially the incident angle, are studied by using Ricker waves (as incident *SH* waves) with different peak accelerations, predominant frequencies and incident angles. A 2-D time-domain nonlinear seismic response analysis code developed by William B. Joyner (William B. Joyner, 1975) is employed throughout this research.

Basin Geometry and Numerical Model

Three symmetrical basins with a simple geometry and shear-wave velocity profile are developed in the present study, as shown in Fig. 1, with L=450m and H=30m, where L and H represent the bottom width, depth respectively, α is the slope angle while θ is the incident angle which is defined as the angle between the incident direction and the vertical direction. In order to investigate the effect of slope angle on the seismic response of a basin, three basins with different slope angles are developed, basin1: α=30°, basin2: α=45°, basin3: α=60°, while the values of both L and H remain constant. These models are shown in Fig. 2. Seven monitoring points are set at the characteristic point of the basin surface. The monitoring points ①②③④ are located on the projection of the midpoint of the basin edge, the left foot point, quarter point of base and midpoint of the base respectively, on the ground. Monitoring point ⑤⑥⑦ are located at the symmetric positions of point ③②① respectively. Bedrock and soil parameters are fixed, as shown in Table 1, the impedance contrast between the sediment and the underlying bedrock is 6.35, and the site classification is class E, according to the seismic site classification standards specified in the International Building Code (IBC, 2012).

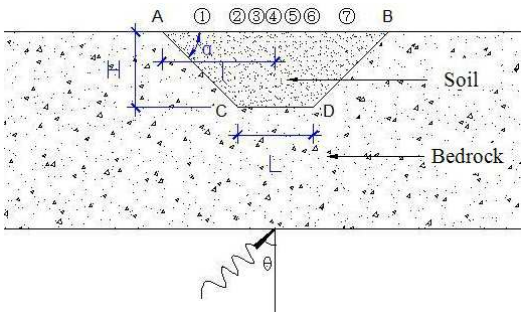

Figure 1. Basin Model

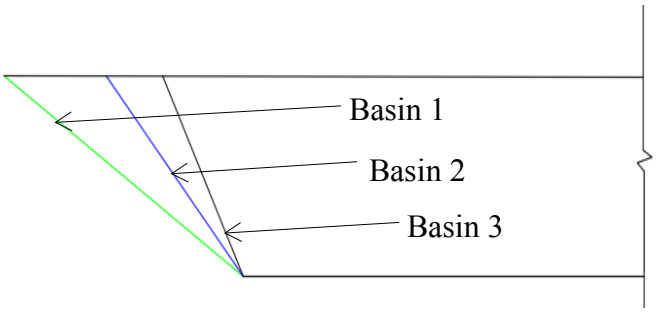

Figure 2. Dimensions of Basin 1, 2 and 3

Table 1. Geotechnical Parameters

Layer	ρ/(Kg/m^3)	V_s(m/s)	H/(m)
Soil	1800.0	175.0	30
Bedrock	2000.0	1000.0	∞

The program used in present study was developed by Willam B. Joyner (William B. Joyner, 1975) for calculating the nonlinear seismic response of 2D configurations of horizontal soil layers resting on a semi-infinite elastic medium representing bedrock. Excitations are shear waves with different incident angles in the underlying medium. The following hyperbolic soil model is implemented to consider the nonlinear, hysteretic and strain-dependent behaviour of soil,

$$\frac{G}{G_{\max}} = \frac{\tau_{\max}}{\tau_{\max} + G_{\max}\gamma} \tag{1}$$

Where G- secant shear modulus, $G = \tau/\gamma$; τ- shear stress; γ- shear strain; τ_{max} - shear strength of the soil, assigned a value 73.9 kPa according to an empirical model (Boore D. M. et al., 1994); G_{max} - elastic shear modulus at small shear strain, $G_{max} = \rho v_s^2$, ρ is the mass density of the soil, and v_s is the soil shear-wave velocity. Fig. 3 shows the reduction of G/G_{max} with increasing shear strain for the selected model, together with models *C1-C5* from Sun (Sun J. et al., 1988), Fig. 4 shows that of damping ratios, together with the upper and lower bound proposed by Seed (Seed, H. B. and Idriss I. M., 1970).Vicious dashpots are placed at the two vertical boundaries and the horizontal boundary so as to permit energy to be radiated back into the underlying half space.

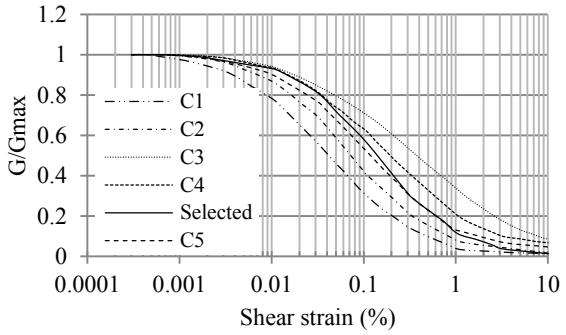

Figure. 3 Modulus vs. shear strain of basin soil

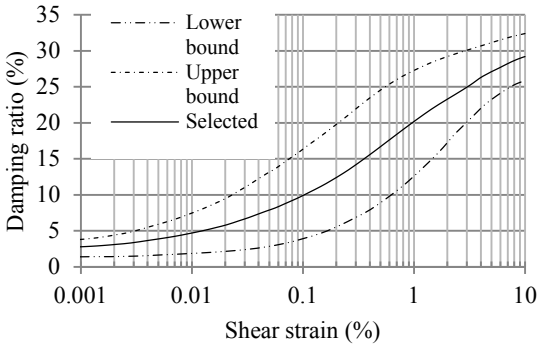

Figure. 4 Damping ratios vs. shear strain of basin soil

The computations are performed by an explicit finite-difference scheme that proceeds step by step in space and time. The reliability of the code has been verified by Willam B. Joyner (William B. Joyner, 1975), the numerical results for a basin illustrated in Fig. 5 by using this program have been compared with those from Boore et al. (Boore D. M. et al., 1971), as shown in Fig. 6. The program employed in this study has been proven to be valid according to the good agreement of these results.

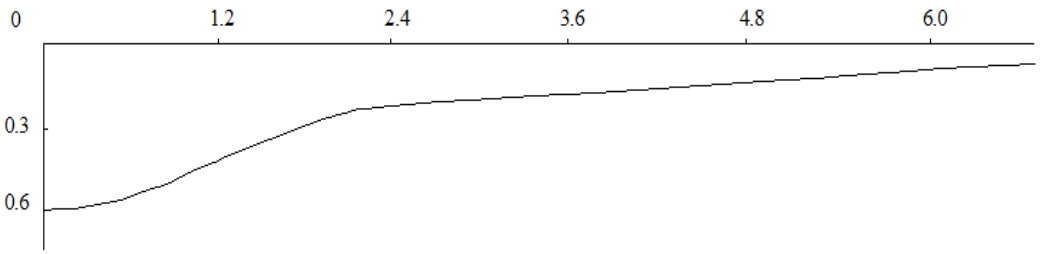

Figure. 5 Symmetrical basin model (unit: km)

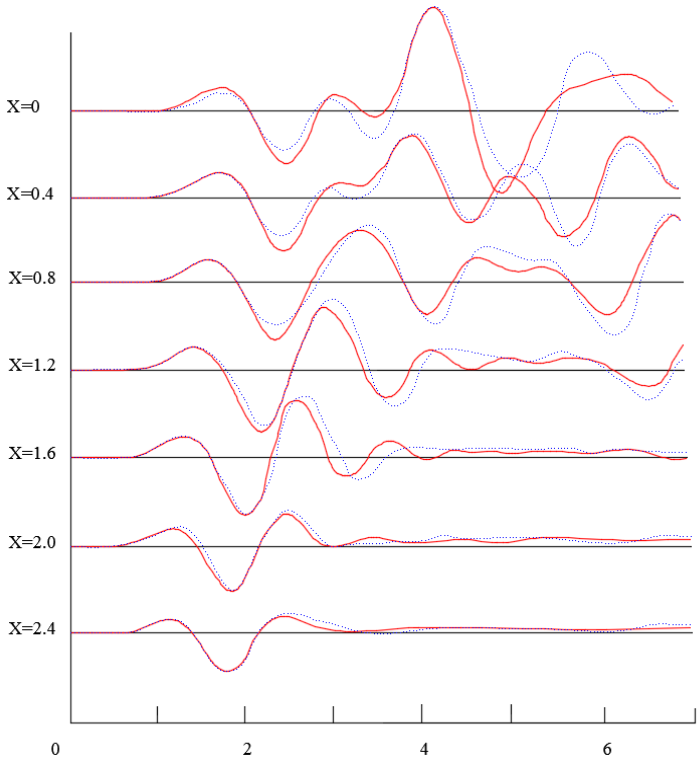

Figure. 6 Horizontal particle displacement with Ricker input, solid lines represent results of the method described in this paper and dotted lines are from Boore et al. (After Willam B. Joyner)

Input Motion

Richer pulses are a type of narrow band waves and are considered to be appropriate for capturing the effect of the predominant frequency. Ricker waves are hence selected as the input *SH* waves. In order to explore the impact of predominant frequency on seismic response, the models are excited by three Ricker waves each with a different predominant frequencies, the predominant frequency of Ricker1 is 1.5*Hz* (being a wave with longer period), that of Ricker3 is 6.5*Hz* (being a wave with shorter period) and Ricker2 is 4.0*Hz*. In order to consider the probable effects of the intensity of input motions, three different amplitudes (0.25*g*, 0.5*g* and 1.0g) for each wave are considered. The acceleration time histories, Fourier spectra and acceleration response spectra of the three Ricker waves (*PGA* = 0.25*g*) are shown in Fig. 7 (a) ~ (c)

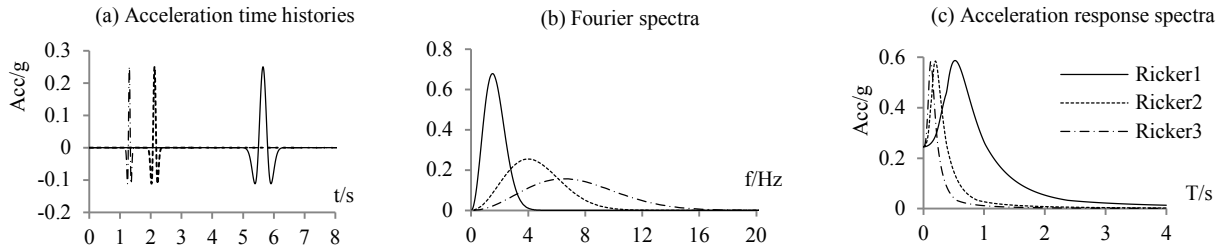

Figure 7 (a) Acceleration time history, (b) Fourier spectra and (c) Acceleration spectra of Ricker 1, 2 and 3

Results and Analysis

Effect of Incident Angle on PGA

Normally only vertically incident seismic waves are used in engineering site assessment. To compare the results for vertically incident case with those for oblique incident ones, the former is selected as a reference to define a dimensionless coefficient $C_i(\theta)$, which is the ratio of the *PGA* calculated under the oblique incident wave (incident angle θ) and that under the vertically incident wave at monitoring point *i*, as follows:

$$C_i(\theta) = \frac{A_i(\theta)}{A_i(0)} \tag{2}$$

Fig. 8(a) ~ (c) illustrates the change of $C_i(\theta)$ with the incident angles for all monitoring points in Basin 2 under Ricker1, Ricker2 and Ricker3 shaking (*PGA*=0.25g) respectively. Fig. 8(a) ~ (c) depicts that the incident angle has a remarkable effect on the seismic response of a basin, and $C_i(\theta)$ greater than 1 indicates that the *PGA* from obliquely incident case is greater than that from vertically incident one. Therefore, it may be unsafe, to some extent, if only the vertically incident case is considered to assess the safety of an engineering site.

With the increase of incident angle, $C_i(\theta)$ increases firstly, then decreases, and eventually tends to be constant. The incident angle corresponding to the maximum $C_i(\theta)$ is defined as the Most Disadvantageous Incident Angle (*MDIA*) in this paper. *MDIA*s at different monitoring points to a given excitation and at a given monitoring point to different excitations are different from each other. *MDIA* can be determined based on the location of a monitoring point and the characteristics of an input motion. Generally, Fig.8 (a) ~ (c) reveal that the *MDIAs* for all monitoring points across the basin are in the range of 0° and 25°.

From the above analyses, it is known that each monitoring point has a certain *MDIA*, and the *MDIA* may not be 0° (namely vertically incident), however, only vertically incident case is considered in seismic safety assessment of engineering sites at present, which may underestimates the intensity of ground motion, shrinking if not exhausting the safety reserve of buildings and infrastructures. Therefore, full attention should be paid to the influence of incident angle in seismic safety assessment practice.

Fig. 8(a) ~ (c) also shows that $C_i(\theta)$ almost remains constant as the incident angle exceeds a certain value. The value is 80°, 65°and 55° for Basin 2 under Ricker1, Ricker2 and Ricker3 shaking (PGA = 0.25g) respectively. It's evident that the value decreases with the increase of the predominant frequency of the input motion, in other words, the range of incident angle that exerts an influence on PGA narrows as the increase of the incident predominant frequency.

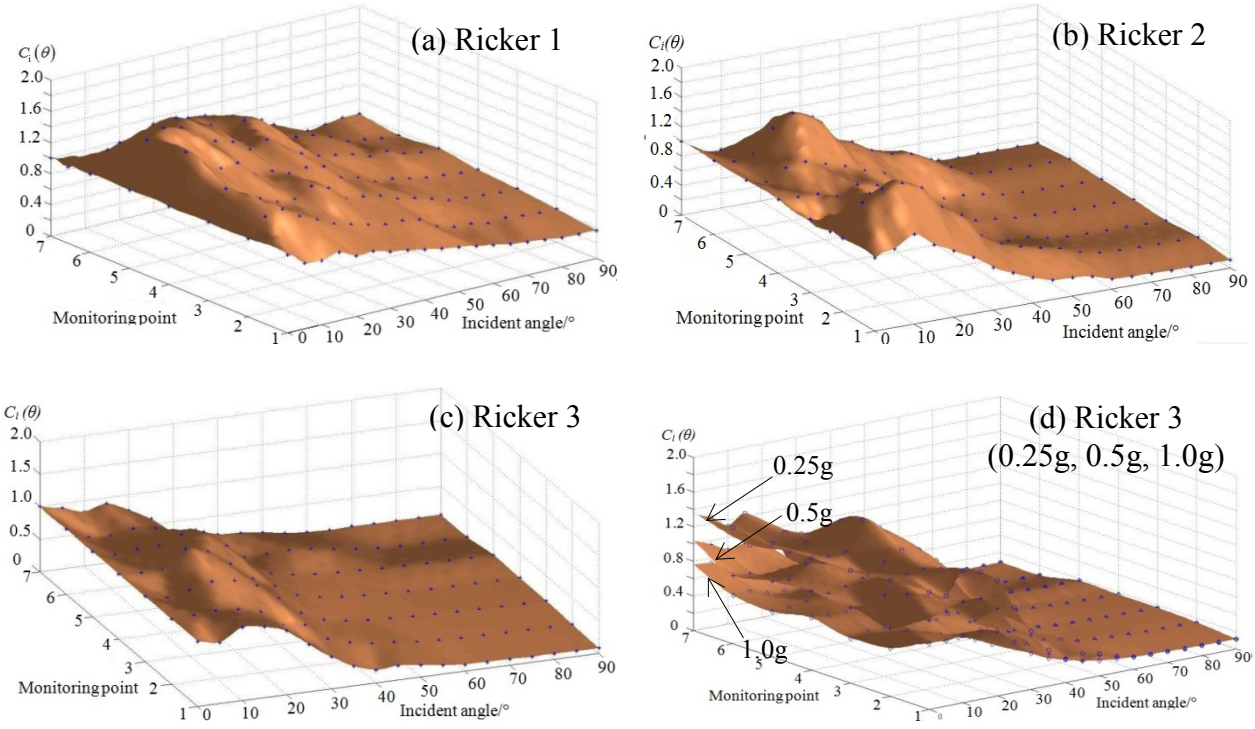

Figure 8. Change of scale coefficient with incident angle for each monitoring point across Basin 2 to (a) Ricker 1, (b) Ricker 2, (c) Ricker 3, and (d) Ricker 3 shaking (PGA=0.25g, 0.5g and 1.0g)

Fig. 8(d) shows the seismic response of Basin 2 under Ricker 3 of which the PGA is 0.25g, 0.5g and 1.0g respectively. A decline is observed in the value of $C_i(\theta)$ with the increase of PGA of incident wave, which suggests the basin undergone a nonlinear seismic response under strong earthquake.

Effect of Incident Angle on Acceleration Spectrum

In order to study the impact of incident angle on the acceleration response spectrum, a given seismic wave incident at different angles was selected. Table 2 depicts the peak value of acceleration response spectra for monitoring points of Basin 1 under Ricker2 shaking (PGA=0.5g) at different incident angles.

Table 2 suggests that the incident angle has an obvious effect on the response spectral of ground motion. As shown in Table 2, with the growth of incident angle, the peak values of response spectra climb first, hit the peak in the range of 0-20°, followed by a steady decline. The trend is similar to that of the $C_i(\theta)$ with the increase of incident angle.

Table 2. Peak of acceleration response spectra for monitoring points of Basin 1 under Ricker2 (*PGA*=0.5g) incident at different angles

Spectrum		Incident angle											
		0°	5°	10°	15°	20°	25°	30°	35°	45°	60°	80°	90°
Point	①	1.4	1.6	**1.69**	1.66	1.55	1.38	1.11	0.8	0.59	0.58	0.5	0.47
	②	0.82	0.84	1.03	**1.07**	1.06	0.99	0.94	0.84	0.63	0.5	0.51	0.51
	③	0.91	0.81	0.89	**1.02**	1.01	0.96	0.92	0.82	0.57	0.48	0.55	0.55
	④	0.94	0.85	0.88	0.95	**0.96**	0.9	0.81	0.75	0.5	0.45	0.51	0.52
	⑤	0.91	0.93	0.86	0.93	**0.96**	0.94	0.82	0.71	0.59	0.43	0.54	0.57
	⑥	0.82	**0.92**	0.9	0.87	0.87	0.87	0.84	0.78	0.71	0.51	0.48	0.48
	⑦	1.4	1.25	1.25	1.3	**1.32**	1.26	1.14	0.93	0.55	0.52	0.55	0.53

Effect of Predominant Frequency on PGA

In order to explore the influences of predominant frequency of input motion on the seismic response, Ricker1, Ricker2 and Ricker3 with the same *PGA* (*PGA*=0.5g) but different predominant frequencies were chosen as the incident *SH* waves. Fig. 9 depicts the change of *PGA*s at monitoring points ① and ② of Basin 2 with the incident angle under Ricker1, Ricker2 and Ricker3 (*PGA*=0.5g). In Fig. 9, the change curves of *PGA* with the incident angle for monitoring points ① and ② increases firstly, prior to a descend, and reaches a plateau. The *MDIA* of monitoring point ① and ② under Ricker1 is 0°, but that under Ricker2 and Ricker3 is in the range of 5° to 15°, which is basically consistent with the range aforementioned.

In Fig.9, the effects of predominant frequency on *PGA* are more complicated when the incident angle is small (< 35 °). Nevertheless, a remarkable downward trend is observed on *PGA* with the increase of predominant frequencies when the incident angle is large (> 35 °). That is, the basin responses more strongly under relatively lower-predominant-frequency seismic waves when the incident angle is large (> 35 °), which can be ascribed to the fact that this lower-predominant-frequency is much close to the fundamental mode of the basin. According to the estimation formula of modal frequencies for the equivalent 1D layered site *f= (2n+1).Vs/4H (n=0, 1, 2….)*, the approximately fundamental frequencies of all the basins developed in this paper are the same-1.46*Hz*, the closer of incident frequency to the fundamental, the more likely to induce resonance.

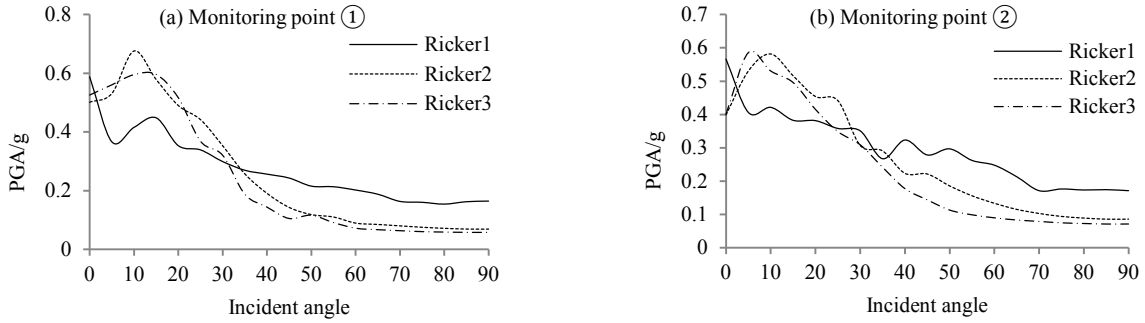

Figure. 9 Effect of incident predominant frequency on *PGA* of monitoring points on Basin 2 to Ricker1, Ricker2 and Ricker3 (*PGA*=0.5g)

Effect of Predominant Frequency on Acceleration Response Spectra

Similarly, Ricker1, Ricker2 and Ricker3 with the same *PGA* (*PGA*=0.5g) are used as input motions to investigate the influence of predominant frequency on acceleration response spectra. Fig. 10 depicts the acceleration response spectra of the monitoring point ③ of Basin 1 under vertically incident Ricker1, Ricker2 and Ricker3 (*PGA*=0.5g). Fig. 10 indicates that the peak of spectral curve gradually "walks" left with the increase of the incident predominant frequency, namely the predominant frequency of spectral acceleration increases with the predominant frequency of input motion.

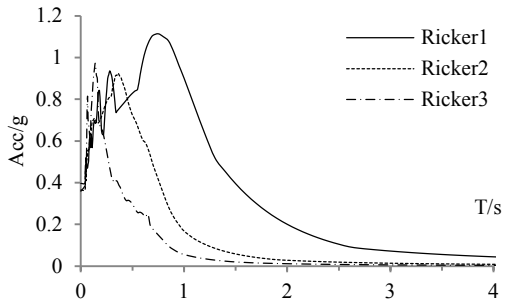

Figure. 10 Acceleration response spectra of monitoring point ③ of Basin 1 to vertically incident Ricker waves (*PGA*=0.5g)

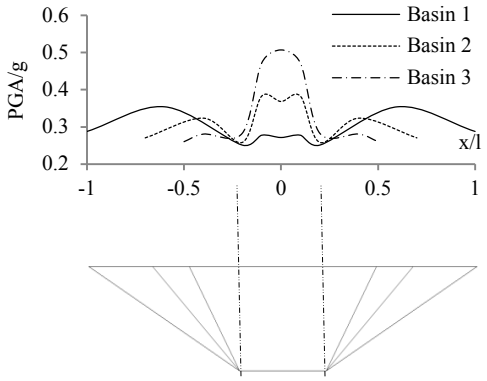

Figure. 11 Distribution of *PGA*s along basins to vertically incident Ricker2 shaking (*PGA* = 0.25g)

Effect of Basin Slope Angle

In order to study the effect of slope angle of basin on the seismic response of a basin, three basins with different slope angles (Basin 1: α=30°; Basin 2: α=45°; Basin 3: α=60°) were developed, and Ricker2 (*PGA*=0.25g, θ=0°) was selected as the incident wave. The distribution of *PGA*s along the surface of the basin is shown in Fig. 11, where *l* is the half-width of basin surface, *x* represents the distance of a site to the midpoint of a basin (right is the positive direction).

Fig. 11 illustrates that the slope angle has a crucial influence on the distribution of *PGA*s across the basin surface. For Basin 1 to the vertically incident Ricker2 (*PGA* = 0.25g), *PGA*s at the triangular wedge are much larger than those at the center and the ends of the basin, Most Disadvantageous Point (*MDP,* the position corresponding to the peak value of *PGA* distribution) located at the basin edges. For Basin 2 under the same incident wave as Basin 1, the *MDP*s locate near the center of the basin. For Basin 3, the distribution of *PGA*s is a smoothed curve with only one peak, with the *MDP* located at the midpoint of the basin. The distribution patterns of the *PGA*s along the basin surface under Ricker1 and Ricker3 are similar to these under Ricker2.

Because of the impact of the slope angle, the distribution patterns of *PGA*s for different basins are different. In order to explore the reason, a simple explanation based on the ray path analysis is presented in Fig. 12. When the slope angle of a basin is small, as shown in Fig. 12(a), the direct incident waves at slope are "trapped" by the wedge-shaped body to some extent, reflected multiply before fleeing. This multiple reflections enhance the possibility of constructive interference in this triangular wedge, thus leading to a strong ground motion in this area. When the slope angle of a basin is large, as shown in Fig. 12(b), the incident seismic waves at slope are reflected directly towards the central region of the basin, hence there is almost no possibility for constructive interference in the wedge-shaped body, yet the interference may happens at the central region of the basin surface since the basin developed in this paper is not broad enough, triggering a stronger ground shaking in the central area of the basin surface.

In summary, the slope angle has a considerable impact on the *PGA* distribution pattern. The *MDP* is most likely to fall in the basin edge area when the slope angle is small. With the increase of the slope angle, the *MDP* gradually transfers towards the central part of the basin surface.

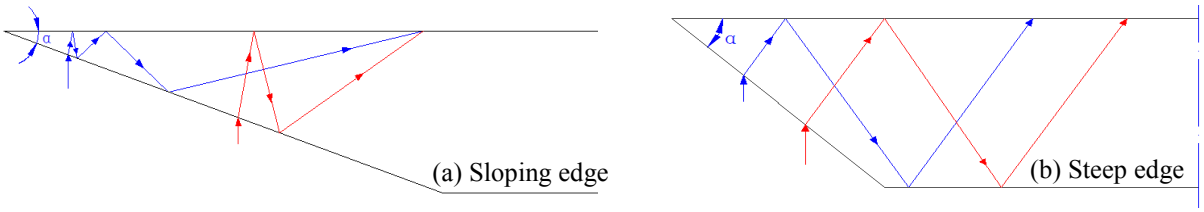

Figure 12. Propagation of seismic waves in basins with different slope angles

Conclusions

In this paper, the impact of incident angle on the seismic response of sedimentary basin was studied by inputting Richer wavelets (as incident *SH* wave) with different peak accelerations, predominant frequencies and incident angles. A total of 513 cases were considered. The following conclusions can be drawn: first, the incident angle of *SH* waves has a significant impact on the ground motion of basin, the *MDIA* is approximately in the range of 0° to 25°. With the increase in incident angle , the peak values of response spectra climb first, hit the peak in the range of 0 ~20°, followed by a steady decline. Second, the increase in the predominant frequency of incident *SH* waves shrinks the range of incident angle that has an effect on *PGA*. At the same time, the spectrum curves gradually "walk" left with the growth of the predominant frequency. Third, the slope angle has an important effect on the *PGA* distribution pattern. Sites at the edge of a basin respond more strongly than that at the middle when the slope angle is small. With the increase of the slope angle, the relatively intensive position gradually transfers towards the middle of the basin.

Acknowledgments

This study is partially sponsored by China Scholarship Council and Queensland University of Technology, I would like to acknowledge their supports for this research.

References

Assimaki, and Gazetas, 2004. Soil and topographic amplification on canyon banks and the 1999 Athens earthquake. *Journal of Earthquake Engineering*, **8**(1):1-43.

Boore et al., 1994. Estimation of response spectra and peak accelerations from Western North American earthquakes: an interim report, Part 2. Open-File Report 94-127, US Geological Survey, Menlo Park.

Boore et al. 1971. Comparison of two independent methods for the solution of wave-scattering problems: Response of a sedimentary basin to vertically incident *SH* waves*, Journal of Geophysical Research*, **76**: 558-569.

Brian et al., 2003. The Basin-Edge Effect from Weak Ground Motions Across the Fault-Bounded Edge of the Lower Hutt Valley, New Zealand, *Bulletin of the Seismological Society of America*, **93** (6) :2703-2716.

Cubrinovski and Green, 2010. Geotechnical reconnaissance of the 2010 Darfield (New Zealand) earthquake. *Report of the National Science Foundation-Sponsored Geotechnical Extreme Events Reconnaissance (GEER) Team*, Report No. GEER-024:180.

Choi et al., 2005. Empirical model for basin effects accounts for basin depth and source location, *Bulletin of Seismological Society of America*, **95**:1412-1427.

Gatmiri and Foroutan, 2012. New criteria on the filling ratio and impedance ratio effects in seismic response evaluation of the partial filled alluvial valleys. *Soil Dynamics and Earthquake Engineering*, **41**: 89-101.

Gelagoti et al., 2012. Nonlinear Dimensional Analysis of Trapezoidal Valleys Subjected to Vertically Propagating SV Waves, *Bulletin of the Seismological Society of America*, **102** (3): 999-1017.

IBC, 2012. International Building Code, International Code Council, INC. ISBN: 978-1-60983-040-3.

Joyner, 1975. A method for calculating nonlinear seismic response in two dimensions. *Bulletin of the Seismological Society of America*, **65**(5): 1337-1357.

Seed and Idriss, 1970. Soil moduli and damping factors for dynamic response analysis, Report No. UCB/EERC-70/10, Earthquake Engineering Research Centre, University of California, Berkeley.

Sun, 1988. Dynamic moduli and damping ratios for cohesive soils. Report No. UCB/EERC-88/15, Earthquake Engineering Research Centre, University of California, Berkeley.

Takahiro, 2000. Estimation of earthquake motion incident angle at rock site. *Proceedings of 12th World Conference Earthquake Engineering*, New Zealand, 956.

Thomas, 2003. Amplification of Seismic Waves by the Seattle Basin, Washington State, *Bulletin of the Seismological Society of America*, **93** (2): 533-545.

You, 2009. Nonlinear seismic response of horizontal layered site due to inclined wave, *Chinese Journal of Geotechnical Engineering*, **31** (2):234-240.

Zhang and Zhao, 2008. Response spectral amplification ratios from 1-and 2-dimensional nonlinear soil site models, *Soil dynamics and Earthquake Engineering*, **29** (3): 563-573.